Environ Geol (2005) 49: 253–266
DOI 10.1007/s00254-005-0083-2

ORIGINAL ARTICLE

Javier Sánchez España
Enrique López Pamo
Esther Santofimia Pastor
Jesús Reyes Andrés
Juan Antonio Martín Rubí

The natural attenuation of two acidic effluents in Tharsis and La Zarza-Perrunal mines (Iberian Pyrite Belt, Huelva, Spain)

Received: 15 April 2005
Accepted: 14 August 2005
Published online: 25 October 2005

J. S. España (✉) · E. L. Pamo
E. S. Pastor
Instituto Geológico y Minero de España (IGME), Dirección de Recursos Minerales y Geoambiente, Rios Rosas, 23, 28003 Madrid, Spain
E-mail: j.sanchez@igme.es
URL:www.igme.es

J. R. Andrés · J. A. M. Rubí
Centro de Laboratorios y Técnicas de Apoyo, La Calera, 1, 28760 Tres Cantos, Spain

Abstract The geochemical evolution of two acid mine effluents in Tharsis and La Zarza-Perrunal mines (Iberian Pyrite Belt, Huelva, Spain) has been investigated. In origin, these waters present a low pH (2.2 and 3.1) and high concentrations of dissolved sulphate and metals (Fe, Al, Mn, Cu, Zn, As, Cd, Co, Cr, Ni). However, the natural evolution of these acidic waters (which includes the bacterial oxidation of Fe(II) and the subsequent precipitation of Fe(III) minerals) represents an efficient mechanism of attenuation. This self-mitigating process is evidenced by the formation of schwertmannite, which retains most of the iron load and, by sorption, toxic trace elements like As. The later mixing with pristine waters rises the pH and favours the total precipitation of Fe(III) at pH 3.5 and, subsequently, Al compounds at pH 4.5, along with the sorption of trace metals (Mn, Zn, Cu, Cd, Co, Ni) until chemical equilibrium at circumneutral conditions is achieved.

Keywords Acid mine waters · Attenuation · Iberian Pyrite Belt · Iron oxidation · Trace metal removal

Introduction and scope

Acid mine drainage (AMD) is an important environmental problem in the province of Huelva (SW Spain). These acidic solutions emerge from mine portals, waste-rock piles and/or tailings ponds in the massive sulphide mines of the Iberian Pyrite Belt (IPB), and transport high quantities of acidity, dissolved sulphate and metals (Fe, Al, Mn, Cu, Zn, Cd, As, Pb, Co, Ni) to creeks, rivers and water reservoirs (Sánchez-España et al. 2004, 2005). In the Odiel river (pH 3.0 ± 0.5), this mine-related pollution implied the transference of more than 3,700 t of dissolved metals (mostly Al, Mn, Zn and Cu, with minor quantities of Fe, Pb, As and Cd) to the Huelva estuary during the year 2003 (Sánchez-España et al. 2005).

The geochemical evolution of these originally anoxic and highly acidic waters is determined by a rapid interaction with atmospheric oxygen, so that dissolved Fe(II) is fastly oxidized to Fe(III) and hydrous iron oxides are formed at pH 3. The hydrolysis of Fe(III) at pH 2–4 usually forms iron oxyhydroxysulphates such as schwertmannite (Bigham et al. 1990, 1996), by the equation:

$$8Fe^{3+} + SO_4^{=} + 14H_2O \Leftrightarrow Fe_8O_8(SO_4)(OH)_6 + 22H^+ \quad (1)$$

The mineralogy of these AMD-related precipitates may include some other mineral phases. Thus, a mixture of schwertmannite ± jarosite ± goethite is recognized in the vicinity of the discharge points at pH 2–4, Al-oxyhydroxysulphate (e.g., hydrobasaluminite) is formed at pH 4–5, and ferrihydrite is present in waters with pH > 6 (Sánchez-España et al. 2005).

The dilution by subsequent mixing with stream courses is an important mechanism by which dissolved metals decrease in concentration. In addition, the

precipitation of ochreous minerals (such as schwertmannite) at pH 2–4, as well as Al-phases at pH > 4, plays an important role in the retention of dissolved SO_4, Fe and Al. Furthermore, these chemical sediments can retain, by sorption and/or coprecipitation, significant amounts of trace elements such as As, Pb, and other metals such as Cu, Zn or Cd. These two processes (precipitation of Fe–Al and dilution) represent a self-mitigating mechanism that attenuates the AMD-related aqueous metal pollution.

The aim of this work was to study the natural attenuation of the mine-related pollution in two mine effluents emerging from some of the largest mine districts in the IPB: Tharsis and La Zarza-Perrunal. The evolution of the water chemistry, as well as the chemical and mineralogical composition of the ochreous precipitates is discussed. Both effluents are chemically distinct (different pH and metal concentrations) but show a similar evolution with two processes clearly differentiated: (1) oxidation of Fe (II) and oxygen-saturation at nearly constant water flow, and (2) progressive dilution with pristine waters, pH increase and neutralisation.

Site description

Although abandoned in the 1990s, both Tharsis and La Zarza-Perrunal were mined since pre-Roman times for the recovery of Ag and Au, and in modern times, for sulphuric acid and metals (Cu, Zn, Pb; Pinedo Vara 1961). These mining areas contain several mine portals, in addition to large waste piles and taillings impoundments. A number of 10 AMD discharges have been recognized in Tharsis, whereas in La Zarza-Perrunal, two effluents emanating from different mine portals have been located (Sánchez-España et al. 2005).

The acid effluents selected for this study are representative of the two most common types of AMD-generating sources in the area (Sánchez-España et al. 2005): (1) leachates emerging from waste-rock piles (50% of the cases recognized in the Odiel basin, exemplified by Tharsis), and (2) outflows from mine portals (30% of the AMD occurrences in the Odiel basin, illustrated by La Zarza-Perrunal). These AMD systems are different as regards to pH and iron concentration. The Tharsis effluent shows a pH of 2.2 and 483 mg/l of Fe, whereas the AMD discharge of La Zarza-Perrunal is less acid (pH 3.1) but more iron-rich (~2,600 mg/l Fe). The stream beds of both effluents are coated by green algal biofilms during the first tens of meters, and then by ochreous precipitates during several kilometers downstream. The location of these mine sites and their hydrologic context is shown in Figs. 1 and 2. The AMD streams are illustrated in Fig. 3.

The Tharsis AMD emerges from the base of a large waste pile situated in the proximity of the Filón Centro pit lake (Fig. 1). This permanent effluent is intersected at a distance of 1,700 m by another AMD discharge coming from an acidic pool (Figs. 1 and 3), and then flows during several kilometers, receiving fresh water from the Molineros, Valdecaballos and Agualobos creeks (Fig. 1). This stream forms the Dehesa Boyal creek and is discharged into the Meca river.

The acid effluent of La Zarza-Perrunal flows at fairly constant flow rate of ~2 l/s during 2.6 km. After receiving some fresh water, this stream meets the Tamujoso creek, and finally, the Tallisca creek, where it is finally neutralized (Fig. 2).

Materials and methods

Sampling and field measurements

Field work was performed on April 2003 (Tharsis) and May 2004 (La Zarza-Perrunal), under low-flow hydrologic conditions. Both effluents were studied downstream, with continuous measurement of pH, Eh, dissolved oxygen (DO) content, electric conductivity (EC) and water flow. To determine the geochemical evolution of the acid waters, different sampling points were established at increasing distance from the respective discharge points. Water samples were taken with 60 ml-syringes and Millipore sampling equipment, filtrated on site through 0.45 μm membrane filters, stored in 125 ml-polyethylene bottles, acidified to pH < 2 with HNO_3, and stored at 4°C. Sediment samples were directly taken and stored in 125 ml-polyethylene bottles.

Field parameters such as pH, Eh, temperature, dissolved oxygen and electric conductivity were measured in situ with HANNA portable instruments properly calibrated against supplied calibration standards. Flow rates were measured with digital flow meters (GLOBAL WATER).

In the study of Tharsis, only a semiquantitative estimation of Fe(II) concentration was performed with Merckoquant® (MERCK) strips. In La Zarza-Perrunal, a more precise iron speciation was determined by colorimetric digital titration (HACH) using citrate as solution buffer, sodium periodate as Fe(II) oxidant, and sulfosalicylic acid as Fe(III) colorimetric detector. The accuracy of this method, calculated by repeated analyses of internal standards, was ±1% in the 100–1,000 mg/l Fe_t range, ±4% in the 50–100 mg/l Fe_t range, and ±12% in the 10–50 mg/l Fe_t range.

Analytical procedures

The AMD samples were analyzed in the IGME laboratories by AAS for Na, K, Mg, Ca, Fe, Cu, Mn, Zn and Al, ICP-AES for Be, Ni and Se, and ICP-MS for As, Cd,

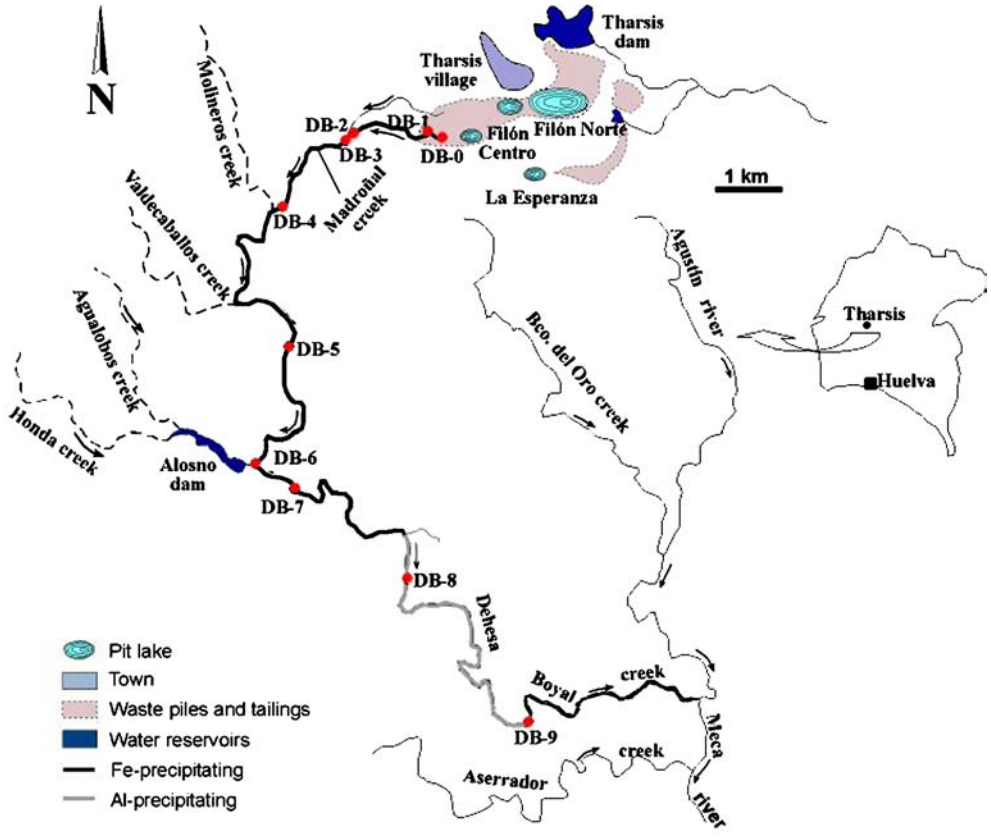

Fig. 1 Location and hydrological configuration of the studied AMD effluent in Tharsis mine (Dehesa Boyal creek)

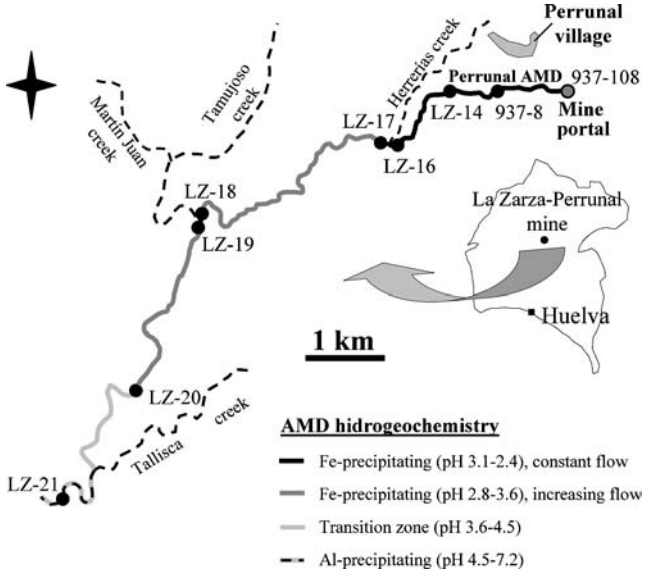

Fig. 2 Location and hydrological configuration of the studied AMD effluent in La Zarza-Perrunal mine (Fuente Perrunal creek)

Co, Cr, Pb, Ni, Th, U and V. Sulphate was gravimetrically measured as $BaSO_4$, whereas chlorine was analyzed titrimetrically with silver nitrate. The accuracy and trueness of the analytical methods were verified against certified reference waters such as SRM 1643 (trace elements in water, NIST), or APG 4073 (trace metals in waste water, APG) and close agreement with certified values was achieved for all metals. Also, ^{115}In was used as internal standard for calibration of the ICP-MS analyses. The detection limit for major cations (Na, K, Ca, Mg, Mn, Fe, Al) was <0.1 mg/l in all cases. The detection limit for trace metals was usually <2 μg/l (Co, Ni, Cr, Pb, Th, U, Se), although it could be locally higher (e.g., 20 μg/l for Cd, 25 μg/l for V, 50 μg/l for Tl).

Solid samples were analyzed using ED-XRF (PANALYTICAL MAGIX) for Si, Al, Fe, Ca, Ti, Mn, K, Mg and P, elemental analyzer (*Eltra CS-800*) for S, ICP-MS (after digestion with HNO_3 and H_2O_2) for Cd, Cr, Ni, V and Zn, and AAS for Na, Cu, As and Pb. Certified international reference materials (BCS 175/2, BCS 302/1, BCS 378, FER-1, FER-2) were used to check the accuracy of the analytical data. The detection limit for trace metals in solids was usually <1 ppm.

Table 1 Field data and chemical analyses of water samples (filtrated through 0.45 μm and unfiltered samples) from the different sampling stations along the Tharsis-Dehesa Boyal mine effluent (see Fig. 1 for location of sampling points)

Sample	Field measurements						Major anions		Major metals				
	Distance (m)	Q (L/s)	pH	Eh (mV)	EC (μS/cm)	DO (% sat.)	SO_4 (g/L)	Cl (g/L)	Na (mg/L)	K (mg/L)	Ca (mg/L)	Mg (mg/L)	Mn (mg/L)
DB-0													
Filtrated	0	2.5	2.2	460	5,560	0	6.01	0.32	19	0.4	123	367	70
Total							5.82	0.31	19	0.4	125	367	70
DB-1													
Filtrated	250	3.2	2.3	509	4,760	90	5.00	0.10	20	0.4	108	313	70
Total							4.93	0.10	20	0.4	108	317	71
DB-2													
Filtrated	1,630	4	2.2	552	3,870	100	3.72	0.09	23	0.6	83	246	51
Total							3.78	0.09	22	0.6	83	245	53
DB-3													
Filtrated	1,730	5.2	2.5	555	3,350	101	3.01	0.13	24	0.7	80	195	42
Total							2.99	0.13	24	0.7	81	198	42
DB-4													
Filtrated	3,560	7	2.3	552	2,690	100	2.11	0.12	25	0.8	58	138	32
Total							2.04	0.12	25	0.8	59	141	32
DB-5													
Filtrated	7,290	9	2.5	536	2,100	102	1.34	0.14	30	1.2	50	102	19
Total							1.47	0.14	30	1.2	50	104	20
DB-6													
Filtrated	9,760	13	2.8	490	1,415	101	0.85	0.11	27	1.6	38	65	13
Total							0.88	0.14	28	1.6	38	70	13
DB-7													
Filtrated	10,900	15	3.1	468	1,112	96	0.61	0.12	30	1.8	33	55	9
Total							0.60	0.12	29	1.8	33	55	9
DB-8													
Filtrated	14,490	20	4.3	320	695	101	0.28	0.13	29	2.1	30	37	5
Total							0.29	0.13	29	2.1	30	36	5
DB-9													
Filtrated	19,260	20	4.8	302	670	98	0.29	0.13	27	2.2	34	39	5
Total							0.28	0.13	27	2.2	33	39	5

The solid samples were characterized by powder XRD using a PHILIPS PW 1710 diffractometer with CuKα radiation (40 kV, 40 mA), and a diffracted-beam monochromator.

Results and discussion

Case study 1: Tharsis mine (Dehesa Boyal creek)

The Tharsis effluent showed a concentration of 483 mg/l of (mostly ferrous) iron, pH 2.2, $T\sim18$°C and a water flow of (2.5 l/s (Table 1). This acidic discharge was primarily anoxic (DO$\sim$0 mg/l) and densely collonized by submerged slime streamers. The effluent was monitored in 10 sampling stations (numbered from DB-0 to DB-9) situated at increasing distance from the discharge point (Fig. 1). The evolution of the aqueous chemistry is given in Table 1, and the chemical and mineralogical composition of sediments is given in Table 2.

Chemical analyses of sulphate and metal ions were coupled with systematic measurement of flow rate to study the downstream evolution of metal loads. As an approach to discriminate between ''dissolved'' (including trully dissolved ions and colloids) and ''particulate'' metal loads, two samples were taken in every sampling point (0.45 μm-filtrated and unfiltrated sample).

Oxidation of Fe(II) and O_2 saturation (0–1,7 km; samples DB-0 to DB-3)

During the first 250 m (DB-0 to DB-1), the geochemical evolution of this effluent is characterized by a rapid equilibration with atmospheric oxygen and mixing with a small acid leachate. The acid effluent evolved from anoxic to nearly oxygen-saturated in only 160 m

Table 1 (Contd.)

					Trace metals									
Fe_t (mg/L)	Fe(II)* (mg/L)	Al (mg/L)	Cu (mg/L)	Zn (mg/L)	As (μg/L)	Cd (μg/L)	Co (μg/L)	Cr (μg/L)	Pb (μg/L)	Th (μg/L)	U (μg/L)	V (μg/L)	TDS (mg/L)	TDL (g/s)
490	~400	426	75	47	108	315	7,306	370	13	15	24	48	7,956	19.89
483	~400	435	75	52	127	342	8,155	468	14	15	24	52	7,767	19.42
322	~100	350	61	45	44	222	5,097	206	119	11	18	25	6,395	20.46
322	~100	356	61	46	44	236	5,228	213	122	11	19	26	6,337	20.28
242	~50	260	48	32	15	74	1,698	78	65	10	18	10	4,797	19.19
245	~50	262	47	32	15	75	1,701	78	68	10	18	10	4,862	19.45
180	~50	194	34	26	12	65	1,553	67	190	7	12	12	3,918	20.37
179	~50	195	35	27	13	65	1,638	72	192	7	18	12	3,904	20.30
98	~50	135	25	19	4	57	1,254	51	226	5	8	8	2,763	19.34
99	~50	137	25	19	5	57	1,285	52	226	4	12	8	2,700	18.90
35	~30	87	15	12	< 1	46	897	28	208	3	6	6	1,831	16.48
36	~30	87	15	12	< 1	46	944	31	207	3	8	6	1,965	17.69
8	~5	53	9	7	< 1	32	562	12	177	1	4	4	1,182	15.36
9	~5	53	9	7	< 1	32	587	13	176	1	6	4	1,249	16.24
3	~3	40	6	5	< 0.5	24	407	7	131	1	3	3	913	13.69
4	~3	56	6	5	< 1	24	410	6	131	1	4	3	920	13.80
0.13	~0	13	3	2	< 0.5	11	200	< 2	45	< 1	1	1	533	10.66
0.14	~0	40	3	2	< 0.5	12	206	< 2	47	< 1	3	1	568	11.35
0.18	~0	11	2	2	< 0.5	10	174	< 2	37	< 1	1	1	542	10.84
0.18	~0	12	2	2	< 0.5	10	174	< 2	37	< 1	1	1	533	10.65

From the apparent discrepancy in the SO_4 and Fe contents between total and filtrated water samples (e.g., $Fe_{total} < Fe_{filtrated}$) an error of around ±3% for SO_4 and around ±1% for Fe, must be assumed

Abbreviations: *Q* approximate water flow (as measured by flow meter); *EC* electric conductivity; *DO* dissolved oxygen; *Fe(II)** semi-quantitative estimation of dissolved ferrous iron (measured with Merckoquant© strips); *TDS* total dissolved solids; *TDL* total dissolved load (TDL = TDS (mg/l) × *Q* (l/s))

(Fig. 4b). This rapid oxygenation favoured the oxidation of Fe(II) (around 75% of the initial content of Fe(II) had been oxidized at only 250 m downstream from the discharge point; Table 1). The oxidation of Fe(II) was reflected in a fast increase of the redox potential from 460 to 552 mV.

The Fe(III) ions formed after Fe(II) oxidation turned the water colour from greenish to reddish, although because of the low pH (~2.2, the limit for Fe(III) hydrolysis; Nordstrom and Alpers 1999), no Fe(III) particles were detected during 0.45 μm-filtration (Table 1). The particle size of schwertmannite is very small (from ~10 nm to 0.5 μm in diameter; Bigham et al. 1996), and it is not retained during filtration through 0.45 μm pore-size. However, the formation of Fe(III) minerals appears to occur in slight proportions, probably favoured by rainfall episodes.

The comparison between filtered and unfiltered samples (Table 1) suggests that Cl, Na, K, Ca, Mg, Th, U and V are not present as particulate load. The differences in SO_4, Fe, Al, Mn, Cu, Zn, As, Cd, Co, Cr and Pb concentration between filtered and unfiltered samples are lower than the analytical variability (±3% for SO_4, ±1% for Fe), and they should not be considered.

As regards to the evolution of the water chemistry, it is concluded that Mg, Mn, Al, Cu, Zn, Th and U behaved conservatively from DB-1 to DB-2, whereas Ca, Na and K were increased, SO_4 and Fe showed slight decreases, and As, Pb, Cr, Co and Cd were considerably decreased (Fig. 5). The observed increase of the Ca, Na and K contents could be the result of either some input of circumneutral water and/or the dissolution of aluminosilicates from the stream bedrock.

Fig. 3 Photographs of some sampling points in the studied effluents: **a** waste pile and acidic effluent in Tharsis as seen from sampling point DB-1; **b** confluence of two acidic effluents in DB-3 (Tharsis); **c** transition from Fe-precipitating (pH 3.1) to Al-precipitating (pH 4.3) aqueous acid solution between DB-7 and DB-8 (Tharsis, Dehesa Boyal creek); **d** aluminous acidic water (pH 4.8) in DB-9; **e** Perrunal mine portal and associated effluent (sample 937–108); **f** schwertmannite-rich laminated formations in the Perrunal effluent in LZ-9; **g** detail of the same schwertmannite-rich laminated formations in the Perrunal AMD system in LZ-11

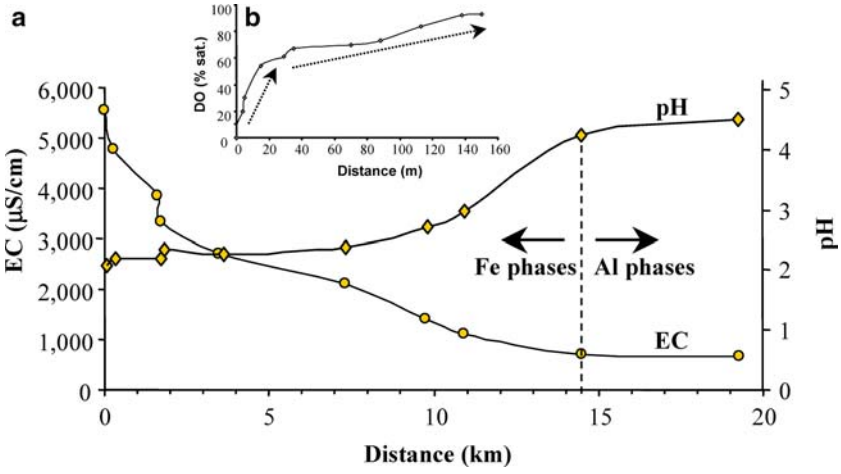

Fig. 4 **a** Spatial evolution of pH and electric conductivity (*EC*) along the 20 km-long segment studied in the Tharsis-Dehesa Boyal AMD system. **b** Detail of the meter-scale evolution of the dissolved oxygen (*DO*) content of the acidic effluent at the discharge point

Metal concentrations decreased from DB-0 to DB-1 and from DB-2 to DB-3 as a result of mixing with other effluents, although the metal load increased in both cases (Table 1, Fig. 5).

Dilution and acidity neutralization (1,7–20 km; samples DB-4 to DB-9)

From DB-4 to DB-9, the evolution of the Dehesa Boyal creek is characterized by a progressive pH increase (from 2.3 to 4.8) and dilution with circumneutral waters (Table 1, Fig. 4a). The attenuation in this segment is not only given by dilution and decrease of metal concentrations, but also by a loss of metal and sulphate loads, which is the result of precipitation of Fe-rich ochreous minerals at pH > 2.5, and then, formation of Al phases at pH > 4 (Figs. 3, 4, 5).

The formation of Fe and Al precipitates in this segment is evidenced in the 0.45 µm filtrates, which retained an increasing percent of the total Fe and Al load at increasing pH (Fig. 6). Thus, the particulate load represented around 1% of the total iron load in DB-4 and 7.2% in DB-7 (Fig. 6a). The Al particulate load was almost zero until DB-6 and 66% in DB-8 (Fig. 6b).

As deduced from Table 1 and Figs. 4, 5, the combined effects of dilution and precipitation represent an important attenuation of this acid effluent. The content of total dissolved solids (TDS) discharged into the Meca river represented only a 6% of the TDS initially transported from the discharge point (~8 g/l in DB-0 and 0.5 g/l in DB-9). The total dissolved load (TDL) was decreased to around a half of the initial load (from ~20 g/s in DB-0 to ~10 g/s in DB-9). The soluble cations Na and K were gradually increased as a result of a continuous input of fresh water (which usually contains 10–20 mg/l Na and 1–3 mg/l K, Sánchez-España et al. 2005) and aluminosilicate dissolution. Conversely, Cl, Mg, Ca, Mn, Th, U and V were conservative, whereas SO_4, Al, Cu, Zn, Cd, and specially, Fe, As, Co and Cr were notably decreased. The loss of SO_4, Fe and Al loads took place by direct precipitation, while the trace elements (As, Cu, Zn, Cd, Co, Cr) would have been sorbed by the Fe and Al hydrous oxides at the pH range 3–5.

Mineralogy and chemistry of the AMD precipitates

The sediments collected along the first 11 km of the studied section (P-DB-1 to P-DB-7) are mainly composed of detritic silicates (quartz, albite, illite, kaolinite) cemented by iron-rich minerals such as schwertmannite and/or goethite (Table 2). These samples show significant

Table 2 Mineralogy and chemical composition of sediments collected in the Tharsis-Dehesa Boyal effluent (see Fig. 1 for location of sampling points)

Sample	Mineralogy (XRD)	Major oxides (wt. %)												Trace metals (mg/kg)							
		SiO_2	Al_2O_3	Fe_2O_3	CaO	TiO_2	MnO	K_2O	MgO	Na_2O	P_2O_5	LOI	Total	As	Cd	Cr	Cu	Ni	Pb	V	Zn
P-DB-1	Qtz, Mc, Schw	37.3	13.6	28.6	0.1	0.6	0.0	2.3	0.1	0.2	0.1	16.8	99.6	717	2	20	299	11	1,015	24	142
P-DB-3	Goet, Qtz, Schw	8.8	4.8	52.3	0.1	0.1	0.1	0.4	0.3	0.1	0.2	33.1	100.3	351	1	19	537	33	127	26	182
P-DB-5	Qtz, Schw, Goet, Mc	20.1	10.5	34.3	0.4	0.3	0.1	1.1	0.9	0.5	0.1	32.7	101.3	164	2	36	803	23	65	38	392
P-DB-6	Schw, Qtz	16.2	5.6	39.8	0.3	0.2	0.1	0.5	1.7	0.4	0.7	37.9	103.3	117	1	35	604	18	71	26	219
P-DB-7	Schw, Qtz	15.8	9.1	40.5	0.2	0.2	0.1	0.9	0.2	0.5	0.1	32.7	100.2	68	b.l.	42	546	29	101	14	73
P-DB-8	Qtz, Al ox., Ka	33.4	24.9	4.9	0.8	0.7	0.1	1.0	0.8	1.0	0.2	32.1	100.0	n.d.	16	37	2,249	20	149	40	402

Abbreviations: *Qtz* quartz; *Mc* muscovite-illite; *Schw* schwertmannite; *Goet* goethite; *Ka* kaolinite; *Al ox.* hydrous Al oxides

Table 3 Field data and chemical analyses of water samples from the different sampling stations along the La Zarza-Perrunal effluent

Sample (Units)	Distance (m)	Field data							Iron speciation				Major ions	
		pH	Eh (mV)	EC (mS/cm)	T (°C)	DO (mg/l)	DO (%)	Q (L/s)	Fe_t (mg/l)	Fe^{2+} (mg/l)	Fe^{3+} (mg/l)	Fe^{2+}/Fe_t (%)	$SO_4^=$ (g/l)	Cl^- (g/l)
937-108	0	3.11	269	7.26	31.0	0.8	10	2	2,675	2,675	0	100	8.84	1.03
LZ-1	9	3.11	269	7.26	28.3	1.6	20	2	2,675	2,640	35	99		
LZ-2	23	3.13	300	7.26	26.8	2.9	36	2	2,615	2,525	90	97		
LZ-3	32	3.12	325	6.81	26.0	4.8	59	2	2,600	2,500	100	96		
LZ-4	82	3.13	346	6.95	23.7	4.1	49	2	2,575	2,450	125	95		
LZ-5	140	3.04	358	6.85	19.5	4.2	42	2	2,450	2,300	150	94		
LZ-6	200	2.96	375	6.65	17.0	4.2	44	2	2,355	2,160	195	92	7.98	1.04
LZ-7	275	2.83	393	6.50	18.3	4.2	45	2	2,260	1,900	360	84		
LZ-8	345	2.80	400	6.41	18.1	5.3	57	2	2,205	1,675	530	76		
LZ-9	415	2.80	405	6.30	18.7	5.3	57	2	2,180	1,650	530	76		
LZ-10	545	2.75	415	6.20	18.1	5.3	57	2	2,000	1,215	785	61	7.20	1.07
LZ-11	645	2.68	424	5.50	18.0	5.2	56	2	1,770	925	845	52		
937-8	900	2.56	448	5.50	18.0	5.4	57	2	1,480	625	855	42	6.54	0.70
LZ-12	1,215	2.53	497	4.71	18.4	5.2	57	2	1,065	150	915	14		
LZ-14	1,545	2.51	542	4.37	17.7	7.9	85	2	935	125	810	13	5.24	0.78
LZ-15	2,295	2.44	543	4.90	18.4	9.4	101	2.3	1,060	120	940	11		
LZ-16	2,605	2.38	583	5.11	18.8	9.6	104	2.3	880	80	800	9		
LZ-17	2,725	2.80	562	1.98	17.6	–	–	10	168	0	168	0		
LZ-18	5,745	2.67	542	1.88	21.2	–	–	15	32	0	32	0	0.89	0.69
LZ-19	5,845	2.91	533	1.27	20.0	–	–	20	20	0	20	0	0.67	0.21
LZ-20	8,355	3.64	420	0.88	19.9	–	–	20	0.7	0	0	0	0.48	0.21
LZ-21	11,705	7.26	490	0.49	17.8	–	–	41	0.03	0	0	0	0.31	0.30

trace metal content (up to 717 ppm As, 2,249 ppm Cu, 1,015 ppm Pb and 402 ppm Zn). Whereas the less soluble metals like As or Pb decrease gradually downstream, the more soluble metals such as Cu and Zn do not show a clear trend.

The samples P-DB-1 to P-DB-7 (with pH < 3.1) always show high iron contents (28–52% Fe_2O_3) and low aluminum concentration (4–13% Al_2O_3), in agreement with the abundance of Fe minerals (schwertmannite, goethite) and scarcity of Al minerals. Conversely, sample P-DB-8 (pH 4.3) showed abundance of amorphous Al compounds and absence of Fe minerals and, accordingly, high Al (~25% Al_2O_3) and low Fe (< 5% Fe_2O_3). The absence of As in sample P-DB-8 is well correlated with the water chemistry of sample DB-8, which shows a virtual absence of As.

Geochemical calculations of saturation indices performed with the PHREEQC program (Parkhurst and Appelo, 1999) are in agreement with the cited chemical and mineralogical observations (Fig. 7). These calculations predict saturation of the acidic solution with respect to schwertmannite, jarosite and goethite from DB-0 to DB-8 (pH < 3.1), and saturation with respect to basaluminite and gibbsite from DB-8 to DB-9 (pH > 4.3). The acidic solution was always undersaturated with respect to ferrihydrite, which has not been observed.

Case study 2: La Zarza-Perrunal mine (Fuente Perrunal creek)

From this mine portal emanates a highly anoxic (< 1 mg/l DO) acid water with very high concentration of ferrous iron (~2.7 g/l Fe(II)). This water showed an initial pH of 3.1, T~31°C and a water flow of 2 l/s which remained fairly constant during 2,600 m. At this point, the AMD intersects a small creek of ~8 l/s and near-neutral pH (Fig. 2). This AMD was monitored in 22 sampling stations (937–108 to LZ-21) situated at variable distance (10–75 m between stations during the first 500 m, and 100–300 m during the subsequent 2 km) until the acidic water was totally neutralized at around 12 km. In addition, a pair of samples was taken upstream and downstream every confluence of the AMD stream with a fresh water course (Fig. 2). Four samples of ochreous precipitates were taken along the segment, being diffractometrically and chemically analyzed (Table 4). These precipitates were essentially formed by schwertmannite.

The downstream variation of the iron speciation and metal concentrations of the La Zarza-Perrunal effluent is given in Table 3. Figure 8 shows the evolution of the iron speciation along the first 2.6 km of the reach, and Fig. 9 illustrates the evolution of metal concentrations.

Table 3 (Contd.)

Major metals								Trace metals							
Na (mg/l)	K (mg/l)	Ca (mg/l)	Mg (mg/l)	Mn (mg/l)	Al (mg/l)	Cu (mg/l)	Zn (mg/l)	As (μg/l)	Be (μg/l)	Cd (μg/l)	Co (μg/l)	Ni (μg/l)	Se (μg/l)	Tl (μg/l)	V
4.7	36	187	412	86	253	21	52	2,280	33	254	1,360	861	111	89	292
4.1	34	200	397	84	249	20	52	754	31	207	1,352	811	95	78	176
3.6	29	199	375	79	234	19	48	264	32	203	1,281	842	78	83	105
2.8	39	206	354	76	220	17	42	< 100	29	181	1,172	815	74	73	59
2.6	39	210	301	64	184	14	34	< 100	28	147	1,020	775	34	< 50	< 25
4.1	49	70	68	10	36	2	5	< 100	5	22	169	130	15	< 50	< 25
3.0	42	53	47	7	25	1.4	3	< 100	3	< 20	103	92	12	< 50	< 25
1.8	39	56	43	5	25	1.2	3	< 100	3	< 20	92	82	4	< 50	< 25
1.0	30	37	21	1	0.1	0.1	0.4	< 100	0	< 20	< 20	13	2	< 50	< 25

Abbreviations: *EC* electric conductivity; *DO* dissolved oxygen; *T* temperature; *Q* approximate water flow (as measured by flow meter); iron speciation measured in situ by colorimetric titration

Oxidation of Fe(II) and O_2 saturation (0–2,6 km; samples 937–108 to LZ-16)

The first 2.6 km of this acidic effluent are characterized by the oxidation of Fe(II), and the subsequent equilibration of water with O_2 at nearly constant flow. Fe(II) was fastly oxidized (and Fe(III) strongly increased) during the first 645 m (Fig. 8). Simultaneously, total iron was progressively decreased due to hydrolysis of Fe(III) ions, which finally provokes the formation and deposition of schwertmannite precipitates on the stream bed. This precipitating process is evidenced along the stream course in the form of cm-thick, laminated formations (Fig. 3f, g), and by a marked pH decrease (see Eq. 1). In the 645 to 1,215 m segment, both Fe(II) and total iron were decreased at the same rate until pH was shifted to 2.5 and Fe(III) concentration was stabilized (Fig. 8). This reflects a steady-state situation balanced by the competing effects of Fe(II) oxidation (H^+-consuming) and Fe(III) precipitation (H^+-releasing).

Assuming a constant flow rate of ~2 l/s during this stream segment, around 94% of the initial Fe(II) had been oxidized to Fe(III) at a distance of 1,215 m, and 60% of the initial total iron load had been removed from solution at 1.5 km, mainly by schwertmannite precipitation (Table 3; Fig. 8). Further, the geochemical evolution showed in Table 3 indicates a decrease of some elements (Fig. 9) which is especially important for As (with a loss of around a 95% at only 900 m from the discharge point) and for V (with a decrease of a 91% at 1.5 km). Other trace metals such as Se and Cd also appear to have been slightly removed from solution.

Table 4 Chemical composition of schwertmannites collected from the La Zarza-Perrunal AMD effluent

Sample N°	Major oxides (wt. %)												Sulphur		Trace metals (mg/kg)											
	SiO_2	Al_2O_3	Fe_2O_3	CaO	TiO_2	MnO	K_2O	MgO	Na_2O	P_2O_5	LOI*	Total	S (%)	$(Fe/S)_{mol}$	Ag	As	Cd	Cr	Cu	Mo	Pb	Sb	Th	Tl	U	V	Zn
P-937-8	1.1	0.7	60.7	0.2	0.0	0.0	0.1	0.1	0.1	0.1	36.8	99.0	–	–	1	742	6	4	91	1	9	4	1	< 0.2	82	83	71
937-109	0.9	0.9	61.8	0.1	0.0	0.0	0.1	0.1	0.1	0.2	35.4	98.7	4.68	5.3	NA	283	< 0.2	26	144	NA	14	6	NA	NA	NA	22	50
LZ-1	0.3	0.4	60.0	0.4	0.0	0.1	< 0.1	0.3	< 0.1	0.2	38.4	99.8	5.84	4.1	41	6,166	1,267	231	55	3	26	6	77	< 2	180	129	211
LZ-2	0.3	0.3	62.2	0.2	0.0	0.0	< 0.1	0.1	< 0.1	0.2	36.5	99.7	5.18	4.8	< 5	1,007	840	22	72	4	7	7	13	< 2	260	133	218

Abbreviations: *NA* not analyzed

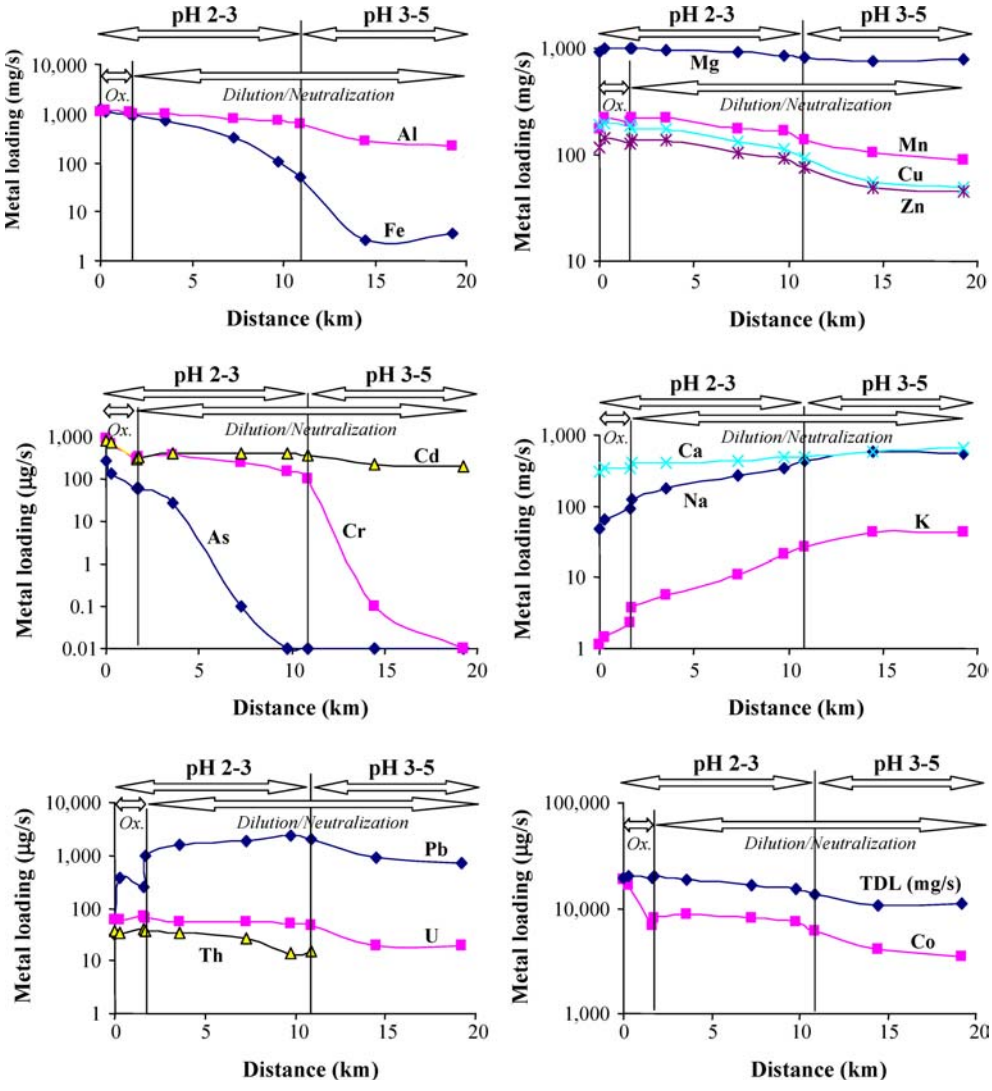

Fig. 5 Evolution of metal loads (metal concentrations [mg/l] × water flow [l/s]) along the Tharsis-Dehesa Boyal AMD system. Two distinct sections are distinguished in the basis of either pH (2–3 and 3–5) and hydrogeochemical evolution of water (Fe(II) oxidation-O_2 saturation (Ox.) and Dilution/Neutralization)

A slight decrease in the concentration of Mg, Mn, Al, Cu, Zn, Co, Ni and Th is also observed in Table 3. These elements are traditionally considered as conservative under acidic conditions. This metal loss could be apparent and provoked by a slight dilution by diffuse water input (not detected in the field). In fact, most of these elements are decreased in around the same proportions (~27% for Mg, Mn and Al, ~33% in the case of Cu and Zn), which points to a hypothetical dilution of around 30% with respect to the initial water volume. Despite this theoretical dilution, Table 3 and Fig. 9 shows that most metalic cations (including Mn, Al, Zn, Cu, Be, Co, Ni and Tl) behaved as essentially conservative during the first 2 km of the stream, and only SO_4, Fe, As and V would have been substantially retained in the solid phase.

The rapid As removal is in agreement with the results reported in other AMD environments (e.g., Leblanc et al. 1996; Fukushi et al. 2003; Casiot et al. 2003). The As retention is achieved by sorption of this element onto colloidal hydrous iron oxides. Under acidic conditions, As, Cr, V and Se usually form oxyanions such as $HAsO_4^{2-}$, $HCrO_4^{2-}$, VO_4^{3-} or SeO_4^{2-} which, as opposed to the cations, show increasing sorption with decreasing pH (Dzombak and Morel 1990; Davis and Kent 1990; Smith 1999). Further, trivalent oxyanions like AsO_4^{3-} or VO_4^{3-} usually form inner-sphere complexes which yield non-reversible sorption edges (Bigham and Nordstrom, 2000). Recently, Regenspurg and Peiffer (2005) have reported important substitutions of sulphate by arsenate and chromate in schwertmannite. Therefore, it could be deduced that both As and V might have been significantly sorbed as oxyanions on the schwertmannite surfaces during the oxidation/precipitation stage.

On the other hand, the sorption of Cu, Zn or Mn on hydrous iron oxides at pH~3 is usually very low (Smith

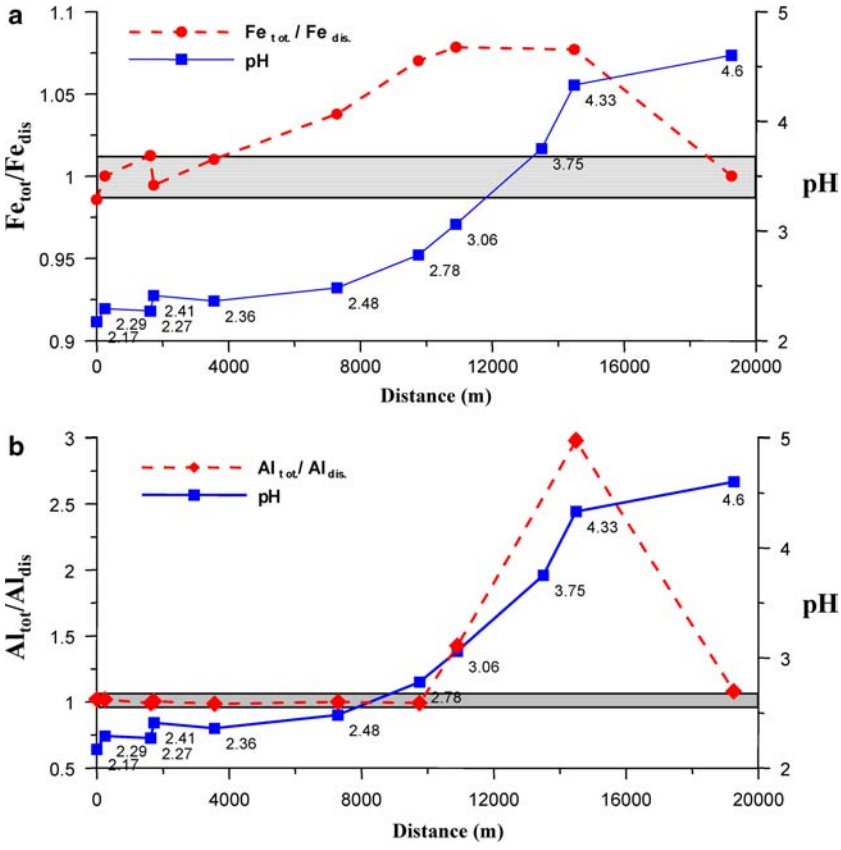

Fig. 6 Evolution of the "particulate" metal loadings (retained by filtration at 0.45 μm) for Fe (**a**) and Al (**b**) along the Tharsis-Dehesa Boyal AMD effluent. Fe_{tot}, total iron (unfiltered sample); Fe_{dis}, "dissolved" iron (filtered sample); Al_{tot}, total aluminum (unfiltered sample); Al_{dis}, "dissolved" aluminum (filtered sample). The *shaded area* indicates the zone of analytical uncertainty within which differences between "dissolved" and particulate metal concentrations are meaningless

1999; Lee et al. 2002). The critical pH range for sorption of divalent cations is commonly comprised between 3 and 5 for Cu, Pb and Hg, 5–6.5 for Zn, Co, Ni and Cd and 6.5–7.5 for Mn (Kinniburgh and Jackson 1981; Smith 1999; Lee et al. 2002). For acid mine waters with pH < 3, these studies predict less than 5% sorption of dissolved metals like Cu, Zn, Ni, Cd or Co. Similarly, Al is fairly conservative at pH below 3 (Nordstrom and Alpers, 1999).

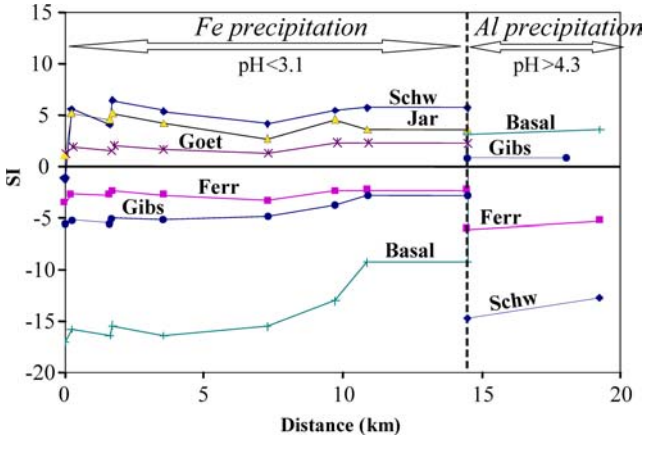

Fig. 7 Evolution of the saturation index (*SI*) of the Tharsis-Dehesa Boyal effluent with respect to different iron and aluminum minerals with increasing distance from the discharge point. The points plotted correspond to the different water samples of Table 1. Positive SI values indicate saturation for a given mineral and thus, precipitation, whereas SI values below 0 indicate subsaturation. Calculations performed with the PHREEQC code (version 2.0; Parkhurst and Appelo 1999). Mineral abbreviations: *Schw* schwertmannite; *Jar* K-jarosite; *Goet* goethite; *Ferr* ferrihydrite; *Gibs* gibbsite; *Basal* basaluminite

The metal content of the four schwertmannite samples taken from this AMD discharge (Table 4) suggests

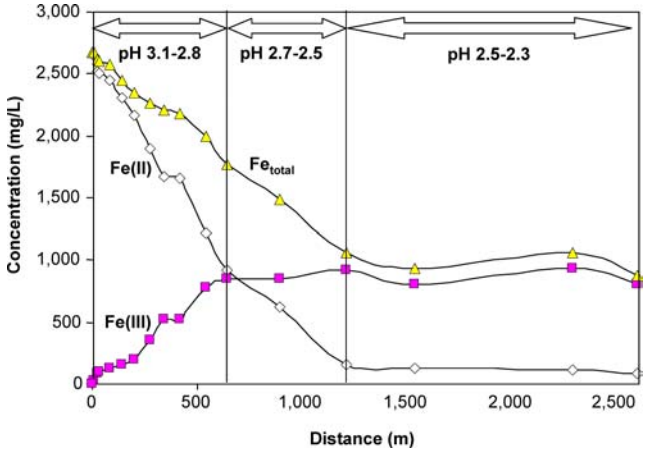

Fig. 8 Evolution of the iron speciation during the first 2.5 km of the La Zarza-Perrunal effluent

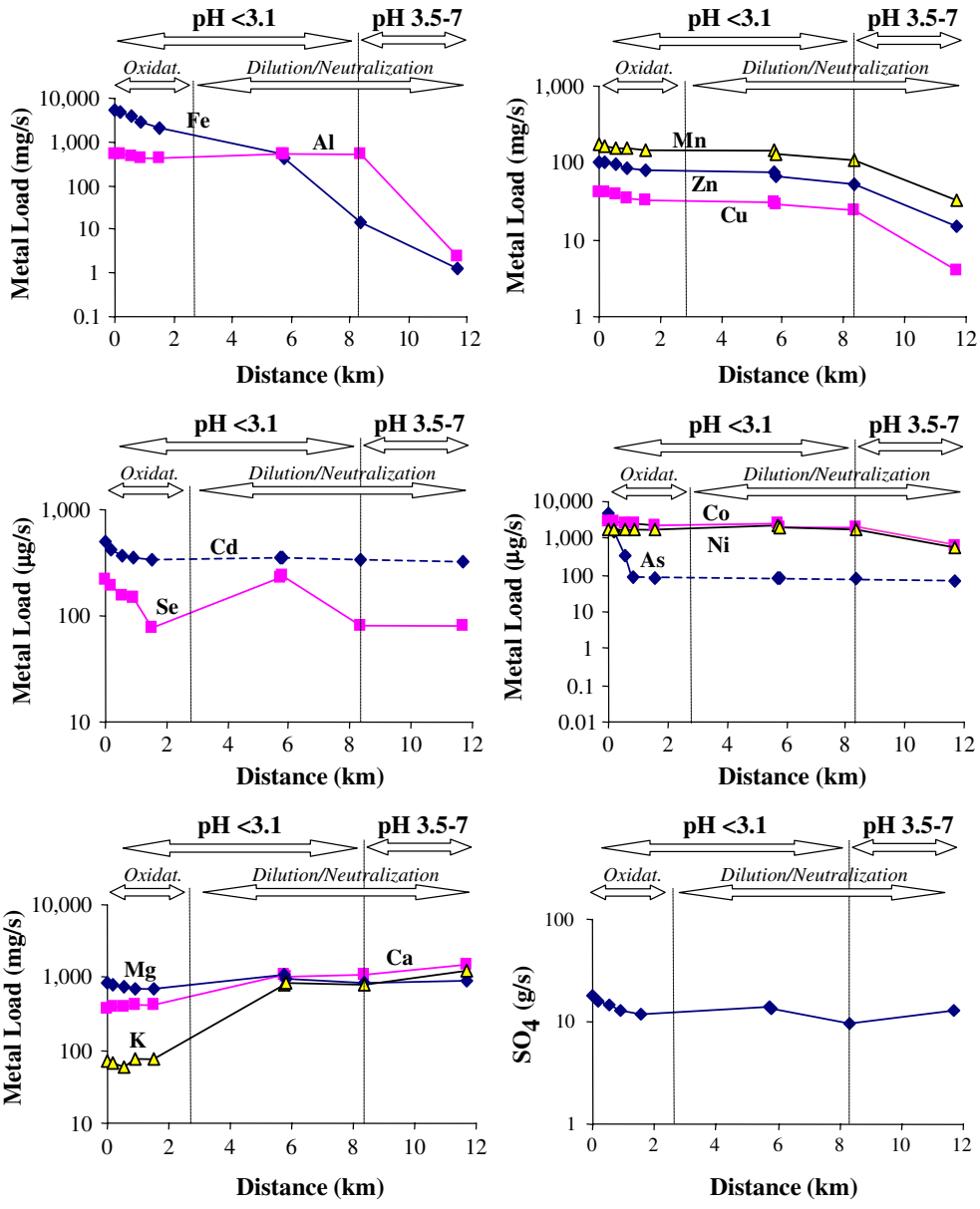

Fig. 9 Evolution of metal and sulphate loads along the La Zarza-Perrunal acidic discharge. Two distinct segments are distinguished in the basis of either pH (< 3.1 and > 3.5) and hidrogeochemical evolution of water (Fe(II) oxidation-O_2 saturation (Oxidat.) and Dilution/Neutralization). The *dotted line* for Cd and As indicates approximate loads considering their corresponding detection limits as concentration values

a strong retention of As, and some degree of Cd sorption on schwertmannite, but a very limited sorption of Cu, Zn and Mn.

Dilution and neutralization (2,7–12 km; samples LZ-17 to LZ-21)

The LZ-17 water sample reflects the mixing of the mine effluent (2.3 l/s) with a neutral water course (8 l/s). This mixing implied a load increase for sulphate and some cations (K, Ca, Mg, Al), although the rest of metals behaved conservatively. This element gain can be explained by either addition of K, Mg and Ca from the pristine stream and/or by redissolution of particulate matter suspended in the clean water course.

Subsequent mixing of this AMD with two streams of circumneutral water (Martín Juan and Tallisca creeks) from LZ-18 to LZ-21 caused the effluent neutralization and a pH shift from 2.7 to about 7.3 (Figs. 2 and 9). This process provoked the complete removal of Fe(III) at pH between 2.7 and 3.6, and then Al at pH > 4–5 (between LZ-20 and LZ-21). Overall, this process represents the loss of around 30% of the sulphate load, and the virtually total loss of metal and acidity loads at 12 km from the mine portal (Table 3, Fig. 9).

As discussed earlier, the removal of iron takes place essentially by schwertmannite precipitation and is virtually complete at pH 3.6. The removal of the rest of metal cations basically occurs between 8.3 and 11.7 km, when pH rises from 3.6 to 7.2, and a total precipitation

of Al takes place mainly at pH > 4.5, probably in the form of nearly amorphous hydrobasaluminite and/or gibbsite. The formation of these minerals (not detected by XRD, but predicted to form by PHREEQC) provokes the total removal of Al and the sorption of most metals (Fig. 9).

Conclusions and final comments

The rapid oxidation of Fe(II) and the subsequent hydrolysis of Fe(III), with precipitation of poorly crystallized minerals such as schwertmannite at pH 2–3, constitutes an efficient mechanism of natural attenuation which reduces considerably the transference of mine-related pollutants (specially Fe and As) to rivers and water reservoirs. The dilution of AMD by mixing with pristine waters provokes an additional decrease of metal concentrations and a progressive pH increase which favours the virtually total precipitation of Fe(III) at pH < 4, and then the removal of Al by formation of poorly crystalline Al phases (hydrobasaluminite, gibbsite) at pH > 4.5. The formation of Fe and Al colloidal precipitates releases acidity and leads to the sorption of considerable amounts of toxic trace elements like As, Pb, Cu, Zn, Cd or Mn.

This natural attenuation is variable, depending on pH and Fe(III) concentration (which essentially determine the amount of sorbent to be formed). Thus, in AMD solutions with pH below 2.5 and moderate Fe concentrations (in the order of tens to hundreds of milligrams per liter), as is the case of the Dehesa Boyal creek (Tharsis), the formation of Fe precipitates is low, and a limited attenuation of metal loads occurs until the AMD is diluted by other water courses. Conversely, at pH > 3 and higher Fe concentrations (in the order of several grams per liter, exemplified by the La Zarza-Perrunal effluent), a more important Fe precipitation favours a stronger attenuation (relative to the initial concentration).

Among the toxic trace elements, As, Cr, V and Se are readily removed from the studied acidic solutions (pH(2.2–3.1) and significantly scavenged at a short distance from the discharge points. On the other hand, the most soluble cations (Cu, Cd, Co, Mn, Zn) remain essentially as dissolved solutes until the pH is raised to near-neutral values, being mostly sorbed in the pH range 4.5–7.5.

Acknowledgements This project was supported with funds from the CICYT project number REN2003-09590-C O4-04, and from Junta de Andalucía (Consejería de Innovación, Ciencia y Empresa).

References

Bigham JM, Nordstrom DK (2000) Iron and aluminum hydroxysulfates from acid sulfate waters. In: Alpers CN, Jambor JL, Nordstrom DK (eds) Sulfate minerals: crystallography, geochemistry, and environmental significance. Rev Mineral Geochem 40:351–403

Bigham JM, Schwertmann U, Carlson L, Murad E (1990) A poorly crystallized oxyhydroxyulfate of iron formed by bacterial oxidation of Fe(II) in acid mine waters. Geochim Cosmochim Acta 54:2743–2758

Bigham JM, Schwertmann U, Traina SJ, Winland RL, Wolf M (1996) Schwertmannite and the chemical modeling of iron in acid sulfate waters. Geochim Cosmochim Acta 60(12):2111–2121

Casiot C, Morin G, Juillot F, Bruneel O, Personné JC, Leblanc M, Duqesne K, Bonnefoy V, Elbaz-Poulichet (2003) Bacterial immobilization and oxidation of arsenic in acid mine drainage (Carnoulés creek, France). Water Res 37:2929–2936

Davis JA, Kent DB (1990) Surface complexation modeling in aqueous geochemistry. In: Hochella MF, White AF (eds) Mineral-water interface geochemistry: reviews in mineralogy. Mineralogical Society of America, Washington, 23:177–260

Dzombak DA, Morel FMM (1990) Surface complexation modeling-hydrous ferric oxide. Wiley, New York, p 393

Fukushi K, Sasaki M, Sato T, Yanese N, Amano H, Ikeda H (2003) A natural attenuation of arsenic in drainage from an abandoned arsenic mine dump. Appl Geochem 18:1267–1278

Kinniburgh DG, Jackson ML (1981) Cation adsorption by hydrous metal oxides and clay. In: Anderson MA, Rubin AJ (eds) Adsorption of inorganics at solid-liquid interfaces; ann arbor science. Ann Arbor, Mich, pp 91–160

Leblanc M, Achard B, Ben Othman D, Luck JM, Bertrand-Sarfati J, Personné JCh (1996) Accumulation of arsenic from acidic mine waters by ferruginous bacterial accretions (stromatolites). Appl Geochem 11:541–554

Lee G, Bigham JM, Faure G (2002) Removal of trace metals by coprecipitation with Fe, Al and Mn from natural waters contaminated with acid mine drainage in the Ducktown Mining District, Tennessee. Appl Geochem 17:569–581

Nordstrom DK, Alpers CN (1999) Geochemistry of acid mine waters. In: Plumlee GS, and Logsdon MJ (eds) The environmental geochemistry of mineral deposits, part A. Processes, Techniques, and Health Issues: Society of Economic Geologists. Rev Econ Geo 6A:33–156

Parkhurst DL, Appelo CAJ (1999) Useŕs guide to PHREEQC (Version 2)—A computer program for speciation, batch-reaction, one-dimensional transport, and inverse geochemical calculations. US Geol Surv Water-Resour Investig Rep 99–4259, Denver-Colorado

Pinedo Vara I (ed) (1961) Piritas de Huelva (su historia, minería y aprovechamiento). Madrid, Summa

Regenspurg S, Peiffer S (2005) Arsenate and chromate incorporation in schwertmannite. Appl Geochem 20:1226–1239

Sánchez-España FJ, López Pamo E, Santofimia E, Aduvire O, Reyes J, Barettino D (2004) Geochemistry and mineralogy of AMD in the Iberian Pyrite Belt (Huelva, Spain). In: Jarvis AP, Dudgeon BA, Younger PL (eds) Proceedings of the MINE WATER 2004 Symposium, vol I, 19–23 September 2004, Newcastle Upon Tyne, England, UK, pp 179–184

Sánchez-España FJ, López Pamo E, Santofimia E, Aduvire O, Reyes J, Barettino D (2005) Acid mine drainage in the Iberian Pyrite Belt (Odiel river watershed, Huelva, SW Spain): geochemistry, mineralogy and environmental implications. Appl Geochem 20(7):1320–1356

Smith KS (1999) Metal sorption on mineral surfaces: an overview with examples relating to mineral deposits. In: Plumlee GS, Losdon MJ (eds) The environmental geochemistry of mineral deposits, Part A. Processes, Techniques, and Health Issues: Society of Economic Geologists. Rev Econ Geol 6A:161–182